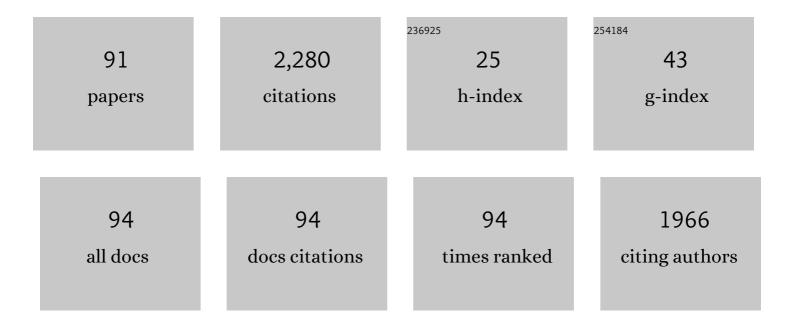
Conrado R M Afonso

List of Publications by Year in descending order

Source: https://exaly.com/author-pdf/1199778/publications.pdf Version: 2024-02-01



#	Article	IF	CITATIONS
1	New insights into the hardening and pitting corrosion mechanisms of thermally aged duplex stainless steel at 475°C: A comparative study between 2205 and 2101 steels. Journal of Materials Science and Technology, 2022, 98, 123-135.	10.7	26
2	Experimental assessment of low-temperature martensite transformations in Ni-rich polycrystalline Ni–Ti alloys. Journal of Materials Research and Technology, 2022, 18, 4990-5004.	5.8	3
3	Anodic growth and pre-calcification on β-Ti-40Nb alloy: Effects on elastic modulus, electrochemical properties, and bioactivity. Ceramics International, 2022, 48, 27575-27589.	4.8	7
4	An exploratory study of TiO2-based multicomponent nanotubes on TiFeNbSn ultrafine eutectic alloy. Surface and Coatings Technology, 2021, 407, 126765.	4.8	3
5	Fundamental studies of magneto-optical borogermanate glasses and derived optical fibers containing Tb3+. Journal of Materials Research and Technology, 2021, 11, 312-327.	5.8	25
6	Impact of Zr content on the nanostructure, mechanical, and tribological behaviors of β-Ti-Nb-Zr ternary alloy coatings. Thin Solid Films, 2021, 721, 138565.	1.8	12
7	Magneto-optical borogermanate glasses and fibers containing Tb3+. Scientific Reports, 2021, 11, 9906.	3.3	23
8	The Effect of Solution Heat Treatment Time on the Phase Formation and Selected Mechanical Properties of Ti-25Ta-xZr Alloys for Application as Biomaterials. Journal of Materials Engineering and Performance, 2021, 30, 5905-5913.	2.5	9
9	Production and characterization of laser cladding coating of Fe66Co7Nb4B23 (at.%) gas-atomized and ball-milled powders. Journal of Materials Research and Technology, 2021, 14, 2267-2280.	5.8	4
10	Assessment of anodization conditions and annealing temperature on the microstructure, elastic modulus, and wettability of β-Ti40Nb alloy. Thin Solid Films, 2021, 737, 138949.	1.8	8
11	Effect of Ni addition on bainite microstructure of low-carbon special bar quality steels and its influence on CCT diagrams. Journal of Materials Research and Technology, 2021, 15, 1266-1283.	5.8	9
12	Severe plastic deformation and different surface treatments on the biocompatible Ti13Nb13Zr and Ti35Nb7Zr5Ta alloys: Microstructural and phase evolutions, mechanical properties, and bioactivity analysis. Journal of Alloys and Compounds, 2020, 812, 152116.	5.5	20
13	Ultrafine eutectic coatings from Fe-Nb-B powder using laser cladding. Materials Characterization, 2020, 160, 110080.	4.4	12
14	New compositions of Fe–Co–Nb–B–Y BMG with wide supercooled liquid range, over 100 K. Journal of Materials Research and Technology, 2020, 9, 9174-9181.	5.8	9
15	Effects of Mg addition on the phase formation, morphology, and mechanical and tribological properties of Ti-Nb-Mg immiscible alloy coatings produced by magnetron co-sputtering. Surface and Coatings Technology, 2020, 400, 126070.	4.8	6
16	Characterization, corrosion resistance and hardness of rapidly solidified Ni–Nb alloys. Journal of Alloys and Compounds, 2020, 829, 154529.	5.5	12
17	Effects of laser surface melting on crystallographic texture, microstructure, elastic modulus and hardness of Tiâ^'30Nbâ^'4Sn alloy. Transactions of Nonferrous Metals Society of China, 2020, 30, 392-404.	4.2	9
18	The Effect of Solution Heat Treatment Temperature on Phase Transformations, Microstructure and Properties of Ti-25Ta-xZr Alloys Used as a Biomaterial. Journal of Materials Engineering and Performance, 2020, 29, 2410-2417.	2.5	13

CONRADO R M AFONSO

#	Article	IF	CITATIONS
19	Effect of friction spot welding parameters on the joint formation and mechanical properties of Al to Cu. Welding in the World, Le Soudage Dans Le Monde, 2019, 63, 33-41.	2.5	11
20	Effect of Thermomechanical Treatments on the Phases, Microstructure, Microhardness and Young's Modulus of Ti-25Ta-Zr Alloys. Materials, 2019, 12, 3210.	2.9	30
21	Characterization of phases, tensile properties, and fracture toughness in aircraftâ€grade aluminum alloys. Material Design and Processing Communications, 2019, 1, e79.	0.9	8
22	Mechanical Properties and the Microstructure of \hat{I}^2 Ti-35Nb-10Ta-xFe Alloys Obtained by Powder Metallurgy for Biomedical Applications. Metals, 2019, 9, 76.	2.3	14
23	Microstructure assessment at high temperature in NiCoCrAlY overlay coating obtained by laser metal deposition. Journal of Materials Research and Technology, 2019, 8, 1761-1772.	5.8	26
24	Slow and rapid cooling of Al–Cu–Si ultrafine eutectic composites: Interplay of cooling rate and microstructure in mechanical properties. Journal of Materials Research, 2019, 34, 1381-1394.	2.6	14
25	Processing, As-Cast Microstructure and Wear Characteristics of a Monotectic Al-Bi-Cu Alloy. Journal of Materials Engineering and Performance, 2019, 28, 1201-1212.	2.5	12
26	Experimental study and thermodynamic computational simulation of phase transformations in centrifugal casting bimetallic pipe of API 5L X65Q steel and Inconel 625 alloy. Journal of Manufacturing Processes, 2018, 32, 318-326.	5.9	11
27	Phosphate glasses <i>via</i> coacervation route containing CdFe ₂ O ₄ nanoparticles: structural, optical and magnetic characterization. Dalton Transactions, 2018, 47, 5771-5779.	3.3	14
28	Microstructural Evolution of HSLA ISO 3183 X80M (API 5L X80) Friction Stir Welded Joints. Metals and Materials International, 2018, 24, 1120-1132.	3.4	12
29	Growth mechanisms of Ca- and P-rich MAO films in Ti-15Zr-xMo alloys for osseointegrative implants. Surface and Coatings Technology, 2018, 344, 373-382.	4.8	46
30	Microstructure characterization of a directionally solidified Mg-12wt.%Zn alloy: Equiaxed dendrites, eutectic mixture and type/ morphology of intermetallics. Materials Chemistry and Physics, 2018, 204, 105-131.	4.0	13
31	A new SERS substrate based on niobium lead-pyrophosphate glasses obtained by Ag+/Na+ ion exchange. Sensors and Actuators B: Chemical, 2018, 277, 347-352.	7.8	13
32	Mechanical and thermal properties of friction-stir welded joints of high density polyethylene using a non-rotational shoulder tool. International Journal of Advanced Manufacturing Technology, 2018, 97, 2489-2499.	3.0	31
33	Nanostructural characterization of sputter deposited Ti-Nb coatings byautomated crystallographic orientation mapping. Thin Solid Films, 2018, 661, 92-97.	1.8	4
34	Effect of Rapid Solidification on Microstructure and Elastic Modulus of β Ti– <i>x</i> Nb–3Fe Alloys for Implant Applications. Advanced Engineering Materials, 2017, 19, 1600370.	3.5	13
35	Influence of Nb content on the structure, morphology, nanostructure, and properties of titanium-niobium magnetron sputter deposited coatings for biomedical applications. Surface and Coatings Technology, 2017, 326, 424-428.	4.8	25
36	From Porous to Dense Nanostructured β-Ti alloys through High-Pressure Torsion. Scientific Reports, 2017, 7, 13618.	3.3	24

CONRADO R M AFONSO

#	Article	IF	CITATIONS
37	An assessment of microstructure and properties of laser clad coatings of ultrafine eutectic \hat{l}^2 Ti-Fe-Nb-Sn composite for implants. Surface and Coatings Technology, 2017, 328, 161-171.	4.8	11
38	On the Process-Related Rivet Microstructural Evolution, Material Flow and Mechanical Properties of Ti-6Al-4V/GFRP Friction-Riveted Joints. Materials, 2017, 10, 184.	2.9	11
39	Laser Cladding of Fe-based Metallic Class/MoS2 Self-lubricating Composites: Effect of Power and Scanning Speed. Materials Research, 2017, 20, 836-841.	1.3	3
40	Metallic Glass Formation Upon Rapid Solidification of Fe60Cr8Nb8B24 (at%) Alloy through LASER Cladding and Remelting. Materials Research, 2017, 20, 580-587.	1.3	9
41	Enhancement of Mechanical Properties of Aluminum and 2124 Aluminum Alloy by the Addition of Quasicrystalline Phases. Materials Research, 2016, 19, 74-79.	1.3	27
42	Effect of Cr Additions on Ferrite Recrystallization and Austenite Formation in Dual-Phase Steels Heat Treated in the Intercritical Temperature Range. Materials Research, 2016, 19, 258-266.	1.3	12
43	Ti-Nb thin films deposited by magnetron sputtering on stainless steel. Journal of Vacuum Science and Technology A: Vacuum, Surfaces and Films, 2016, 34, .	2.1	18
44	Assessment of microstructure of alloy Inconel 686 dissimilar weld claddings. Journal of Alloys and Compounds, 2016, 684, 628-642.	5.5	48
45	Effect of thermal aging at 475 °C on the properties of lean duplex stainless steel 2101. Materials Characterization, 2016, 114, 211-217.	4.4	45
46	Microstructural and mechanical properties analysis of extruded Sn–0.7Cu solder alloy. Journal of Materials Research and Technology, 2015, 4, 84-92.	5.8	19
47	Influence of phase transformations on dynamical elastic modulus and anelasticity of beta Ti–Nb–Fe alloys for biomedical applications. Journal of the Mechanical Behavior of Biomedical Materials, 2015, 46, 184-196.	3.1	50
48	Microstructure development and mechanical properties of rapidly solidified Ti–Fe and Ti–Fe–Bi alloys. Materials and Design, 2015, 86, 221-229.	7.0	14
49	Effects of composition and heat treatment on the mechanical behavior of Ti–Cu alloys. Materials & Design, 2014, 55, 1006-1013.	5.1	77
50	Formation of Fe-based glassy matrix composite coatings by laser processing. Surface and Coatings Technology, 2014, 240, 336-343.	4.8	56
51	Au and Pd nanoparticles supported on CeO 2 , TiO 2 , and Mn 2 O 3 oxides. Applied Surface Science, 2014, 315, 490-498.	6.1	19
52	Nonlinear Optical Properties of Tungsten Lead–Pyrophosphate Glasses Containing Metallic Copper Nanoparticles. Plasmonics, 2013, 8, 1667-1674.	3.4	37
53	Microstructure evolution and mechanical properties of Al–Zn–Mg–Cu alloy reprocessed by spray-forming and heat treated at peak aged condition. Journal of Alloys and Compounds, 2013, 579, 169-173.	5.5	67
54	New insight on the solidification path of an alloy 625 weld overlay. Journal of Materials Research and Technology, 2013, 2, 228-237.	5.8	142

Conrado R M Afonso

#	Article	IF	CITATIONS
55	Microstructure study of Al 7050 alloy reprocessed by spray forming and hot-extrusion and aged at 121°C. Intermetallics, 2013, 43, 182-187.	3.9	25
56	Formation and microstructure of Ni62- x Nb38Ti x (x = 3, 6, 10 at.%) bulk metallic glasses. International Journal of Materials Research, 2012, 103, 1096-1101.	0.3	5
57	Rapid solidification of an Al-5Ni alloy processed by spray forming. Materials Research, 2012, 15, 779-785.	1.3	8
58	Aspectos metalúrgicos de revestimentos dissimilares com a superliga à base de nÃquel inconel 625. Soldagem E Inspecao, 2012, 17, 251-263.	0.6	27
59	Study of La2â^xCaxCuO4 perovskites for the low temperature water gas shift reaction. Applied Catalysis A: General, 2012, 413-414, 85-93.	4.3	22
60	Electrochemical corrosion behavior of gas atomized Al–Ni alloy powders. Electrochimica Acta, 2012, 69, 371-378.	5.2	19
61	Amorphous phase formation by spray forming of alloys [(Fe0.6Co0.4)0.75B0.2Si0.05]96Nb4 and Fe66B30Nb4 modified with Ti. Journal of Alloys and Compounds, 2011, 509, S148-S154.	5.5	13
62	Microstructure of directionally solidified Ti–Fe eutectic alloy with low interstitial and high mechanical strength. Journal of Crystal Growth, 2011, 333, 40-47.	1.5	24
63	Effects of double aging heat treatment on the microstructure, Vickers hardness and elastic modulus of Ti–Nb alloys. Materials Characterization, 2011, 62, 673-680.	4.4	87
64	Microstructure, corrosion behaviour and microhardness of a directionally solidified Sn–Cu solder alloy. Electrochimica Acta, 2011, 56, 8891-8899.	5.2	87
65	Correlations between aging heat treatment, ω phase precipitation and mechanical properties of a cast Ti–Nb alloy. Materials & Design, 2011, 32, 2387-2390.	5.1	57
66	Hexagonal martensite decomposition and phase precipitation in Ti–Cu alloys. Materials & Design, 2011, 32, 4608-4613.	5.1	55
67	Characterization of Glass Forming Alloy Fe _{43.2} Co _{28.8} B _{19.2} Si _{4.8} Nb ₄ Processed by Spray Forming and Wedge Mold Casting Techniques. Materials Science Forum, 2011, 691, 23-26.	0.3	7
68	Fracture toughness of ISO 3183 X80M (API 5L X80) steel friction stir welds. Engineering Fracture Mechanics, 2010, 77, 2937-2945.	4.3	64
69	High resolution transmission electron microscopy study of the hardening mechanism through phase separation in a β-Ti–35Nb–7Zr–5Ta alloy for implant applications. Acta Biomaterialia, 2010, 6, 1625-1629.	8.3	74
70	Effect of the addition of Ta on microstructure and properties of Ti–Nb alloys. Journal of Alloys and Compounds, 2010, 504, 330-340.	5.5	39
71	Microstructural characterization of a laser remelted coating of Al91Fe4Cr3Ti2 quasicrystalline alloy. Scripta Materialia, 2009, 61, 709-712.	5.2	28
72	Effect of cooling rate on Ti–Cu eutectoid alloy microstructure. Materials Science and Engineering C, 2009, 29, 1023-1028.	7.3	71

#	Article	IF	CITATIONS
73	Aging response of the Ti–35Nb–7Zr–5Ta and Ti–35Nb–7Ta alloys. Journal of Alloys and Compounds, 2007, 433, 207-210.	5.5	85
74	Influence of cooling rate on microstructure of Ti–Nb alloy for orthopedic implants. Materials Science and Engineering C, 2007, 27, 908-913.	7.3	118
75	Spray forming of glass former Fe63Nb10Al4Si3B20 alloy. Materials Science & Engineering A: Structural Materials: Properties, Microstructure and Processing, 2007, 449-451, 884-889.	5.6	23
76	In-situ crystallization of amorphous Fe73â^'xNbxAl4Si3B20 alloys through synchrotron radiation. Journal of Non-Crystalline Solids, 2006, 352, 3404-3409.	3.1	12
77	Soft Magnetic Properties of Amorphous Fe _{73-x} Nb _x Al ₄ Si ₃ B ₂₀ Alloys. Journal of Metastable and Nanocrystalline Materials, 2005, 24-25, 431-434.	0.1	0
78	Gas Atomization of Nanocrystalline Fe ₆₃ Nb ₁₀ Al ₄ Si ₃ B ₂₀ Alloy. Journal of Metastable and Nanocrystalline Materials, 2004, 20-21, 175-182.	0.1	4
79	Spray forming of the glass former Fe83Zr3.5Nb3.5B9Cu1 alloy. Materials Science & Engineering A: Structural Materials: Properties, Microstructure and Processing, 2004, 375-377, 571-576.	5.6	14
80	Amorphous phase partitioning in FeCo-based metallic glass alloys. Journal of Non-Crystalline Solids, 2004, 348, 250-257.	3.1	15
81	Microstructure of Spray Formed Fe ₈₃ Nb ₄ ZrTiB ₉ Cu ₂ Alloy. Materials Science Forum, 2003, 416-418, 388-394.	0.3	3
82	Microstructural Characterization of Spray Deposited Al-Y-Ni-Co-Zr Alloy and Al-Y-Ni-Co-Zr + SiC _p Metal Matrix Composite. Materials Science Forum, 2002, 403, 95-100.	0.3	2
83	Amorphous phase formation during spray forming of Al84Y3Ni8Co4Zr1 alloy. Journal of Non-Crystalline Solids, 2001, 284, 134-138.	3.1	30
84	Amorphous phase formation in spray deposited AlYNiCo and AlYNiCoZr alloys. Scripta Materialia, 2001, 44, 1625-1628.	5.2	35
85	Effects of Composition on Solidification Microstructure of Cast Titanium Alloys. Materials Science Forum, 0, 649, 183-188.	0.3	8
86	Effects of Cooling Rate and Sn Addition on the Microstructure of Ti-Nb-Sn Alloys. Solid State Phenomena, 0, 172-174, 190-195.	0.3	11
87	Overspray Powder Characterization of Fe-Based Glassy Alloy. Materials Science Forum, 0, 727-728, 468-475.	0.3	3
88	Evaluation of the Corrosion Resistant Weld Cladding Deposited by the TIG Cold Wire Feed Process. Materials Science Forum, 0, 783-786, 2822-2827.	0.3	5
89	Rapid Solidification and Laser Cladding of Gas Atomized Ni-Nb-Sn Bulk Metallic Glass. Materials Science Forum, 0, 899, 311-316.	0.3	2
90	Effect of Fe Addition on Microstructure and Properties of Powder Metallurgy Ti35Nb10Ta Alloy. Materials Science Forum, 0, 899, 206-211.	0.3	2

#	Article	IF	CITATIONS
91	CARACTERIZAÇÃ ${ m f}$ O MICROESTRUTURAL DA INTERFACE DE TUBO BIMETÃ ${ m L}$ ICO CENTRIFUGADO. , 0, , .		0